Protonation of Metal−Metal Bonds in Dinuclear Iridium Complexes: Consequences for Structure and Reactivity

D. Michael Heinekey,* David A. Fine, and David Barnhart

Department of Chemistry, Box 351700, University of Washington, Seattle, Washington 98195-1700

Received December 30, 1996[⊗]

Protonation of the carbonyl-bridged dimer $[Cp^*Ir(\mu\text{-}CO)]_2$ ($Cp^* = \eta^5\text{-}C_5Me_5$) (**1**) with 1 equiv of the strong acid $HBAr'_4{\cdot}2Et_2O$ ($Ar' = 3,5\text{-}(CF_3)_2C_6H_3$) generates the hydride- bridged species $\{[Cp^*Ir(CO)]_2(\mu\text{-}H)\}BAr'_4$ (**2**). Addition of excess acid to **1** results in the formation of the dihydride dication $[Cp^*Ir(CO)]_2(\mu\text{-}H)_2^{2+}$ (**3**). The monoprotonated cation, **2**, reacts rapidly with CO or H_2 to afford $[Cp^*Ir(CO)]_2(\mu\text{-}CO)(\mu\text{-}H)^+$ (**4**) and $[Cp^*Ir(CO)H]_2(\mu\text{-}H)^+$ (**5**), respectively. The structures of the cationic dimers **4** and **5** have been confirmed by X-ray diffraction studies. Deprotonation of complex **5** generates the neutral dihydride dimer $[Cp^*Ir(CO)H]_2$ (**6**), a compound with an unsupported Ir−Ir bond. An X-ray diffraction analysis of **6** reveals an Ir−Ir bond length of 2.730(1) Å. Formal protonation of the Ir−Ir bond of **6** to give **5** results in an increase of approximately 0.198 Å in the length of that bond.

Introduction

There is an extensive body of work devoted to the chemistry of cyclopentadienyl carbonyl dimers possessing multiple bonds between the metal atoms.[1] Dimers of the form $[(\eta^5\text{-}C_5R_5)M(CO)]_2$ (M = Co, Rh, Ir; R = H, Me) contain a formal M═M double bond, according to electron counting convention, and the carbonyls adopt bridging positions. The Cp* iridium dimer $[Cp^*Ir(\mu\text{-}CO)]_2$ (**1**) was first reported by Graham and co-workers[2] as a byproduct of photolysis reactions of $Cp^*Ir(CO)_2$. An efficient synthesis of **1** was only achieved quite recently,[3] via thermolysis of $Cp^*Ir(CO)_2$ in 1-butanol at reflux.

Hoffmann[4] has used molecular orbital arguments to suggest that these compounds, $[(\eta^5\text{-}C_5R_5)M(CO)]_2$, are isolobal with ethylene. This approach has been successfully exploited by a number of research groups to prepare new compounds.[5] For example, analogous to the cyclopropanation of ethylene, addition of diazoalkanes to these unsaturated metal dimers provides an efficient route to bridging alkylidenes. Heinekey and Michel[6] have shown that reaction of **1** with CH_2N_2 in THF at 195 K affords the metallacyclopropane complex $[Cp^*Ir(CO)]_2(\mu\text{-}CH_2)$ (eq 1).

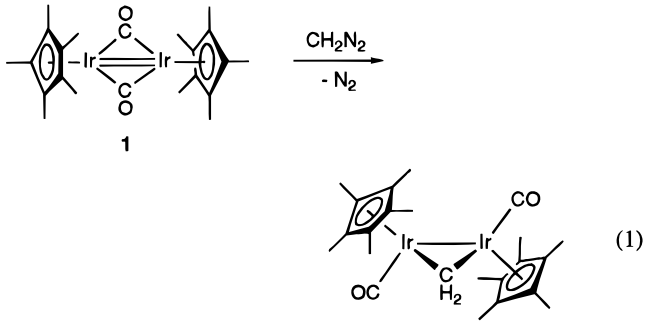

(1)

An obvious extension of ethylene chemistry would be reaction of unsaturated cyclopentadienyl carbonyl metal dimers with electrophiles, such as hydrogen halides (or any proton donor), though there are surprisingly few examples. Curtis and co-workers[7] performed a variety of electrophilic additions to the Mo−Mo triple bond of $Cp_2Mo_2(CO)_4$ ($Cp = \eta^5\text{-}C_5H_5$), including oxidative addition of HX (X = Cl, I) to generate the hydride-bridged complexes $Cp_2Mo_2(CO)_4(\mu\text{-}H)(\mu\text{-}X)$ (formal Mo−Mo single bond).

Recently, we investigated[8] the structure and dynamics of a dinuclear dihydride complex of iridium $[Cp^*Ir(CO)H]_2$ (**6**), which was synthesized via acid-induced condensation of two molecules of $Cp^*Ir(CO)H_2$. Since the preparation and manipulation of $Cp^*Ir(CO)H_2$ are somewhat difficult due to its low melting point and extreme air sensitivity, we sought an alternative route to dimeric iridium hydrides. The carbonyl-bridged dimer, **1**, is an air-stable compound with a strong Ir−Ir bond[6] and appears to be a good platform for the preparation of dimeric derivatives. However, exposure of a solution of **1** to hydrogen gas does not afford the dihydride dimer, **6**, but instead results only in slow fragmentation to $Cp^*Ir(CO)H_2$.[9] In this paper, we report that protonation of **1** with 1 equiv of a strong acid substantially increases the reactivity of the dimer and

[⊗] Abstract published in *Advance ACS Abstracts,* May, 15, 1997.

(1) For a review of unsaturated cyclopentadienyl carbonyl dimers, see: Winter, M. J. *Adv. Organomet. Chem.* **1989**, *29*, 101.

(2) Graham, W. A. G.; Hoyano, J. K.; McMaster, A. D. Presented at the 23rd International Conference on Coordination Chemistry, Boulder, CO, 1984; TH51.

(3) Ball, R. G.; Graham, W. A. G.; Heinekey, D. M.; Hoyano, J. K.; McMaster, A. D.; Mattson, B. M.; Michel, S. T. *Inorg. Chem.* **1990**, *29*, 2023.

(4) Hoffmann, R. *Angew. Chem., Int. Ed. Engl.* **1982**, *21*, 711.

(5) For example, see: (a) Herrmann, W. A.; Krüger, C.; Goddard, R.; Bernal, I. *Angew. Chem., Int. Ed. Engl.* **1977**, *16*, 334. (b) Clauss, A. D.; Dimas, P. A.; Shapley, J. R. *J. Organomet. Chem.* **1980**, *201*, C31. (c) Green, M.; Mills, R. M.; Pain, G. N.; Stone, F. G. A.; Woodward, P. *J. Chem. Soc., Dalton Trans.* **1982**, 1309.

(6) Heinekey, D. M.; Michel, S. T.; Schulte, G. K. *Organometallics* **1989**, *8*, 1241.

(7) Curtis, M. D.; Fotinos, N. A.; Han, K. R.; Butler, W. M. *J. Am. Chem. Soc.* **1983**, *105*, 2686.

(8) Heinekey, D. M.; Fine, D. A.; Harper, T. G. P.; Michel, S. T. *Can. J. Chem.* **1995**, *73*, 1116.

(9) Fine, D. A. Ph.D. Thesis, University of Washington, Seattle, WA, 1996.

S0276-7333(96)01103-X CCC: $14.00

leads to the efficient preparation of a variety of dimeric hydride derivatives.

Results

Monoprotonation of [Cp*Ir(μ-CO)]$_2$ (1): Generation of [Cp*Ir(CO)]$_2$(μ-H)$^+$ (2). A variety of strong acids protonate [Cp*Ir(μ-CO)]$_2$ (**1**), including HOTf (OTf = OSO_2CF_3, triflate), HBF_4·Et_2O, HBAr′$_4$·2Et_2O, and $H_2C(SO_2CF_3)_2$, but not HCl. Addition of 1 equiv of HBAr′$_4$·2Et_2O to a solution of **1** in methylene chloride causes an immediate color change from yellow to dark blue-green. ^{1}H NMR spectroscopy reveals new resonances in the Cp* (δ 1.95) and hydride regions (δ −17.97) in a ratio of 30:1. An IR spectrum of the isolated dark blue solid (Nujol mull) exhibits an absorbance at 1994 cm^{-1}, characteristic of a terminal CO stretch,[10] but no peaks attributable to a terminal or bridging hydride.[11] Significantly, reaction of the dihydride dimer [Cp*Ir(CO)H]$_2$ (**6**) with the hydride abstraction reagent, [Ph_3C]BAr′$_4$ (1.1 equiv), in CD_2Cl_2 similarly results in the bright yellow solution turning deep blue-green. A ^{1}H NMR spectrum again displays new resonances at δ 1.95 and −17.97, with concomitant formation of Ph_3CH. On the basis of these data and on its subsequent reactivity (vide infra), we formulate the product of these two reactions as {[Cp*Ir(CO)]$_2$(μ-H)}BAr′$_4$ (**2-BAr′$_4$**).

Addition of HBF_4·Et_2O or HOTf to solutions of complex **1** in methylene chloride also generates the monoprotonated dimer, **2**, though not as cleanly. Analysis of both reactions by ^{1}H NMR spectroscopy reveals several unidentified resonances in the Cp* region. In the case of reaction with HBF_4·Et_2O, a resonance in the Cp* region at 2.11 ppm corresponds to a hydride resonance at −14.87 ppm that integrates as 15:1. These resonances are tentatively assigned to the dihydride dication {[Cp*Ir(CO)]$_2$(μ-H)$_2$}(BF_4)$_2$ (**3-BF$_4$**) (vide infra). Protonation of **1** with HBF_4·Et_2O or HOTf also results in precipitation of red solids.

Combination of HCl and **1** in CD_2Cl_2 results in neither color change nor reaction, as determined by ^{1}H NMR spectroscopy.

Diprotonation of [Cp*Ir(μ-CO)]$_2$ (1): Generation of [Cp*Ir(CO)]$_2$(μ-H)$_2^{2+}$ (3). Reverse addition of a CH_2Cl_2 solution of **1** to an excess of HBF_4·Et_2O (9.5 equiv) in CH_2Cl_2 produces a pale orange solution containing a suspension of fine red solids. An IR spectrum of the isolated solid as a Nujol mull exhibits a single strong absorbance in the CO region at 2052 cm^{-1}, which we assign as a terminal CO stretch. No peak corresponding to a terminal or bridging Ir−H vibration was observed. NMR spectroscopy of the solid was attempted in a variety of solvents but was generally uninformative due to either the material's insolubility or reactivity with the solvent. As mentioned above, the material appears to be sparingly soluble in CD_2Cl_2.

The reaction of **1** with an excess of HBAr′$_4$·2Et_2O (4.3 equiv) in CD_2Cl_2 causes the solution to become deep blue-green upon thawing and subsequently red-brown after shaking for 1−2 min. The ^{1}H NMR spectrum indicates that the starting material is completely consumed and that the main product possesses resonances at δ 2.10 and −15.23 in a 15:1 ratio. From this and the IR spectrum of the isolated BF_4^- analogue, we formulate the structure of the product of **1** and excess HBAr′$_4$·2Et_2O or HBF_4·Et_2O as the diprotonated dication {[Cp*Ir(CO)]$_2$(μ-H)$_2$}X$_2$ (X = BF_4, BAr′$_4$) (**3**). Addition of the base 1,8-bis(dimethylamino)naphthalene (Proton Sponge, 1 equiv) to **3-BAr′$_4$** in CD_2Cl_2 regenerates {[Cp*Ir(CO)]$_2$(μ-H)}BAr′$_4$ (**2-BAr′$_4$**), confirming the formulation of the dihydride dication.

Reactions of [Cp*Ir(CO)]$_2$(μ-H)$^+$ (2). Strong evidence for the formulation of the monoprotonated dimer as [Cp*Ir(CO)]$_2$(μ-H)$^+$ (**2**) is provided by its reactivity with CO, H_2, and Cl^- to afford known compounds (see Scheme 1). Addition of CO to a solution of [Cp*Ir(μ-CO)]$_2$ (**1**) and HBAr′$_4$·2Et_2O in CD_2Cl_2 rapidly generates {[Cp*Ir(CO)]$_2$(μ-CO)(μ-H)}BAr′$_4$ (**4-BAr′$_4$**), identified by comparison to the chemical shifts of the $HC(SO_2CF_3)_2^-$ salt.[6] A structural determination of the OTf^- salt (**4-OTf**) was made by single-crystal X-ray diffraction (vide infra). The carbonyl- and hydride-bridged dimer **4** has been prepared previously[6] by the addition of the acid $H_2C(SO_2CF_3)_2$ to [Cp*Ir(CO)]$_2$(μ-CO) in methylene chloride.

When H_2 is added to CD_2Cl_2 solutions of isolated **2-BAr′$_4$** or in situ with **1** and HBAr′$_4$·2Et_2O the dark blue-green color is replaced by a golden yellow. The product is identified as {[Cp*Ir(CO)H]$_2$(μ-H)}BAr′$_4$ (**5**) by comparison to an authentic sample prepared by reaction of the oxidant [Cp_2Fe]BAr′$_4$ with Cp*Ir(CO)H_2.[9] Deprotonation of **5** with 1,8-bis(dimethylamino)naphthalene generates the neutral dihydride dimer [Cp*Ir(CO)H]$_2$ (**6**).[8] Structural determinations of **5** and **6** were obtained by single-crystal X-ray diffraction (vide infra).

The addition of [PPN]Cl (PPN = $(PPh_3)_2N^+$) to a CD_2Cl_2 solution of **2** results in deprotonation of the hydride-bridged dimer and regeneration of **1**, along with the formation of HCl. Deprotonation of **2** by the very weak base Cl^- is consistent with the inability of HCl to protonate **1**.

X-ray Crystallographic Analysis of {[Cp*Ir(CO)]$_2$(μ-CO)(μ-H)}OTf (4-OTf), {[Cp*Ir(CO)H]$_2$(μ-H)}BAr′$_4$ (5), and [Cp*Ir(CO)H]$_2$ (6). A summary of the crystallographic data is presented in Table 1. ORTEP diagrams are shown in Figures 1−3. Selected bond lengths and angles are given in Table 2. Atomic coordinates with thermal parameters are provided in the Supporting Information.

Discussion

MonoProtonation of [Cp*Ir(μ-CO)]$_2$ (1). Addition of proton donors to unsaturated metal dimers of the form [Cp′M(CO)]$_2$ (Cp′ = Cp, Cp*; M = Co, Rh, Ir) has not been previously reported. However, the ability of **1** to react with small electrophiles was not wholly unexpected based on previous work by Heinekey and Michel. In 1989, it was reported[6] that Me^+ (in the form of MeOTf) added across the Ir═Ir double bond of **1** to generate {[Cp*Ir(CO)]$_2$(μ-CH_2)(μ-H)}OTf (eq 2).

(10) Infrared absorbances for terminal carbonyl ligands occur from 2125 to 1850 cm^{-1}, see: Collman, J. P.; Hegedus, L. S.; Norton, J. R.; Finke, R. G. *Principles and Applications of Organotransition Metal Chemistry*; University Science Books: Mill Valley, CA, 1987.

(11) Terminal hydride ligands give rise to IR bands in the range from 2200 to 1600 cm^{-1} and bridging hydrides from 1400 to 800 cm^{-1}, see: Kaesz, H. D.; Saillant, R. B. *Chem. Rev.* **1972**, *72*, 231.

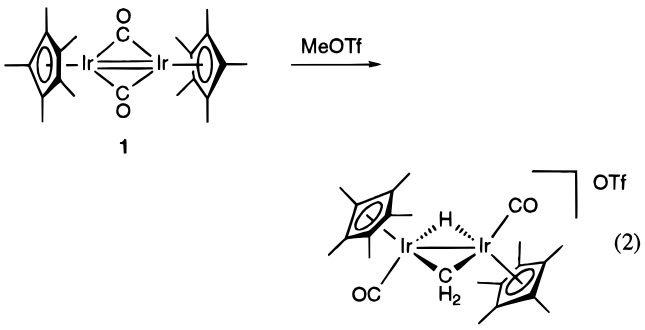

1 (2)

Table 1. Summary of Crystal Data for {[Cp*Ir(CO)]$_2$(μ-CO)(μ-H)}OTf (4), {[Cp*Ir(CO)H]$_2$(μ-H)}BAr′$_4$ (5), and [Cp*Ir(CO)H]$_2$ (6)

	4	5	6
formula	$C_{24}H_{31}F_3Ir_2O_6S$	$C_{54}H_{45}BF_{24}Ir_2O_2$	$C_{22}H_{32}Ir_2O_2$
color; habit	orange; needle	green; trapezoid	yellow; needle
cryst size (mm)	0.1 × 0.1 × 0.1	0.12 × 0.28 × 0.40	0.1 × 0.1 × 0.3
cryst syst	monoclinic	triclinic	orthorhombic
space group	$P2_{1/n}$	$P\bar{1}$	*Pbca*
a (Å)	7.790(1)	12.873(3)	15.107(2)
b (Å)	25.572(3)	21.209(4)	16.165(2)
c (Å)	14.080(2)	22.364(4)	17.853(3)
α (deg)	67.02(3)		
β (deg)	105.36(2)	86.61(3)	
γ (deg)		83.91(3)	
V (Å^3)	2703.1(14)	5589(3)	4359.9(1)
Z	4	4	8
fw	889.0	1577.2	712.9
ρ_{calcd} (g/cm^3)	2.182	1.856	2.172
μ (mm^{-1})	9.970	4.878	12.209
F(000)	1676	2980	2672
radiation	Mo Kα (λ = 0.710 73 Å)		
temp (K)	183	183	183
monochromator	highly oriented graphite crystal		
2θ range (deg)	1.0−50.0	2−45	2.0−50.0
scan type	ω	ω	2θ−ω
scan range (ω)	$0.80 + 0.35(\tan\theta)°$		
no. of rflns collctd	6361	15 318	4127
no. of indep rflns	4752	14 536	3817
no. of obs rflns[a]	3515	10 793	2275
no. of params refined	326	1496	236
abs corr	empirical	semi-empirical	semi-empirical
R_F; R_{wF} (%)	3.58; 4.60	4.48; 6.51	3.75; 4.55
goodness of fit	1.14	1.11	1.04

[a] $F > 4.0\sigma(F)$.

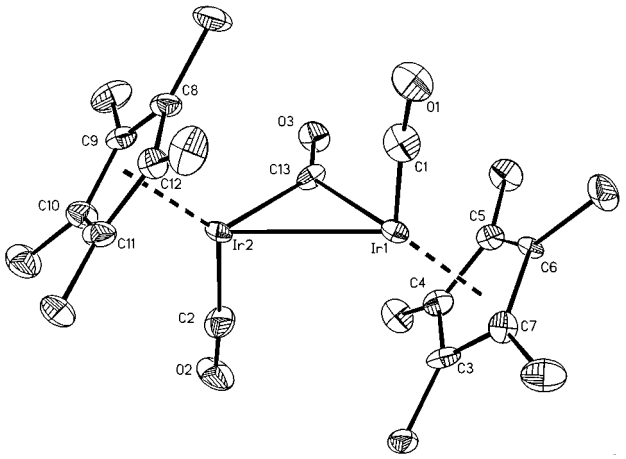

Figure 1. ORTEP representation of {[Cp*Ir(CO)]$_2$(μ-CO)(μ-H)}OTf (**4**). Thermal ellipsoids are shown at 50% probability. Hydrogen atoms are omitted for clarity. The OTf$^-$ anion is not pictured.

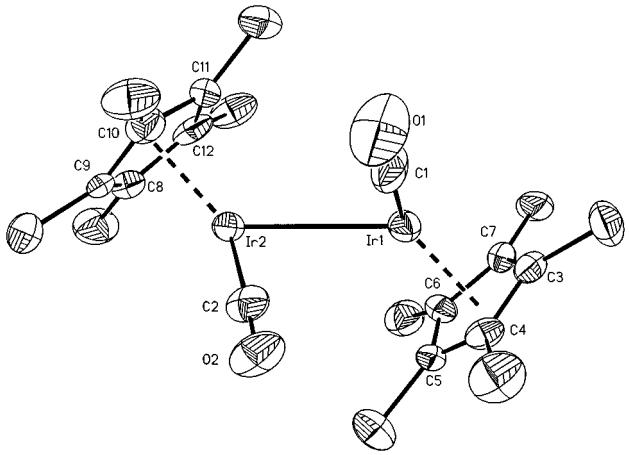

Figure 2. ORTEP representation of {[Cp*Ir(CO)H]$_2$(μ-H)}BAr′$_4$ (**5**). Thermal ellipsoids are shown at 50% probability. Hydrogen atoms are omitted for clarity. The BAr′$_4^-$ anion is not pictured.

Despite possessing a formal Ir═Ir double bond, **1** is not a good base: strong acids are required to effect proton transfer. In fact, **1** is not protonated by HCl. This was confirmed by reaction of {[Cp*Ir(CO)]$_2$(μ-H)}BAr′$_4$ (**2-BAr′$_4$**) with [PPN]Cl, which leads to deprotonation of the dimer and formation of HCl. These experiments suggest that in CH_2Cl_2, HCl is a weaker acid than HBAr′$_4$·2Et$_2$O. This result is corroborated by Cowie and co-workers[12] who found that protonation of a cationic diphosphine-bridged iridium hydride dimer [Ir$_2$(H)(CO)$_2$(μ-H)$_2$(dppm)$_2$]BF$_4$ to generate the tetrahydride dication can be accomplished by protonated ether (HBF$_4$·Et$_2$O) but not by HCl.

The molecular orbital description of **1** is consistent with its poor basicity. The electrons of the two HOMOs are not localized between the metal atoms, but instead are stabilized by delocalization over the bridging carbonyls. The two molecular orbitals that are metal−metal bonding ($1a_g$ and $4b_u$) are best described as 4-center, 2-electron bonds. The construction of these frontier orbitals was first carried out by Hoffmann and co-workers[13] using extended Hückel calculations, and their shape, symmetry, and relative ordering were confirmed by Griewe and Hall[14] using Fenske-Hall methods. This description is also supported by photoelectron spectroscopy.[14]

Transfer of a proton to **1** greatly enhances the reactivity of the metal−metal bond. Infrared data suggest that the bridging carbonyls have swung open into terminal positions, reducing steric congestion at the Ir−Ir bond, and the hydride adopts a bridging position, forming a 3-center, 2-electron bond. The single IR carbonyl stretch is consistent with that predicted for a trans geometry with an idealized C_{2h} symmetry (ignoring the bridging hydride). The independence of the Cp* and hydride ^{1}H NMR chemical shifts of {[Cp*Ir(CO)]$_2$(μ-H)}X (**2**) with various anions is evidence that the counterion is noncoordinating. The transformation of the carbonyls from bridging to terminal positions upon protonation is well-documented in related systems. Bursten and co-workers,[15] in a series of papers on the

(12) McDonald, R.; Sutherland, B. R.; Cowie, M. *Inorg. Chem.* **1987**, *26*, 3333.

(13) Pinhas, A. R.; Hoffmann, R. *Inorg. Chem.* **1979**, *18*, 654.
(14) Griewe, G. L.; Hall, M. B. *Organometallics* **1988**, *7*, 1923.

Scheme 1

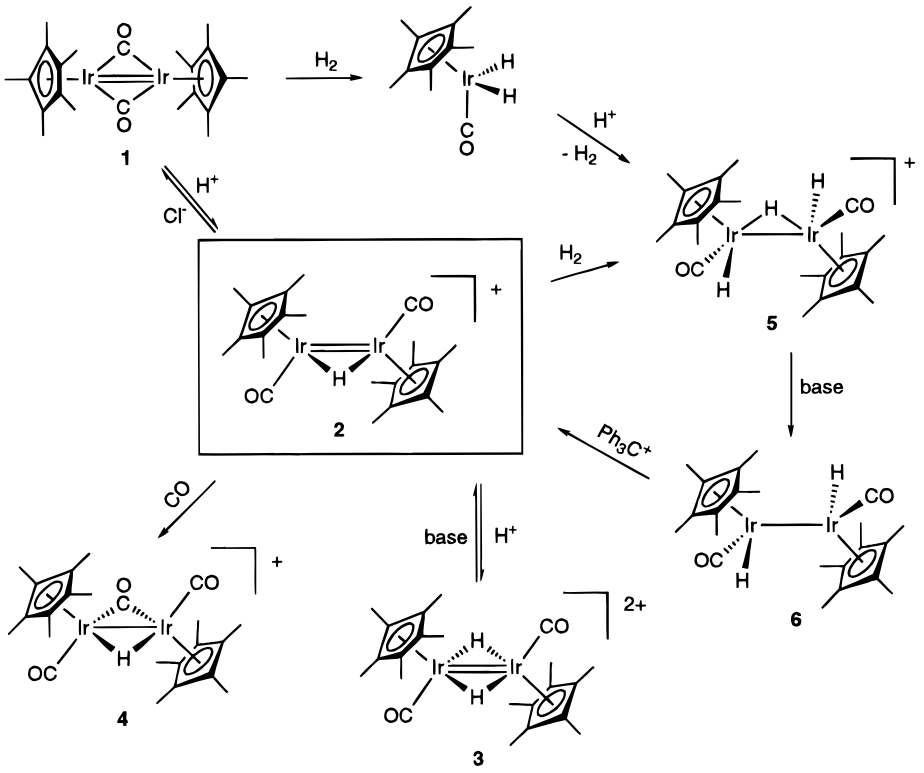

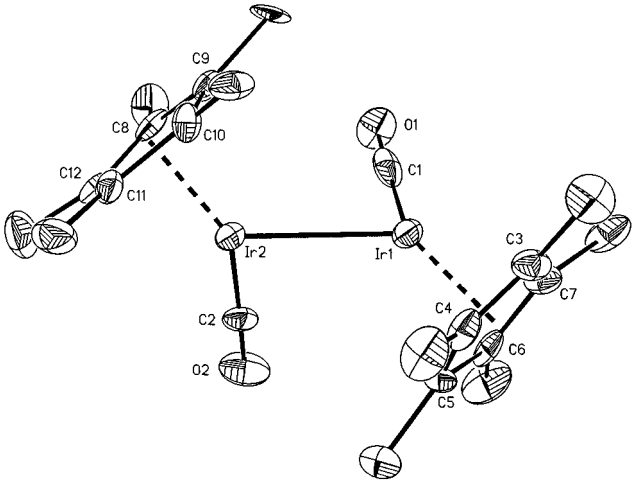

Figure 3. ORTEP representation of $[Cp^*Ir(CO)H]_2$ (**6**). Thermal ellipsoids are shown at 50% probability. Hydrogen atoms are omitted for clarity. The hydride ligands were not located.

Table 2. Selected Bond Distances and Angles for {$[Cp^*Ir(CO)]_2(\mu$-CO)(μ-H)}OTf (4), {$[Cp^*Ir(CO)H]_2(\mu$-H)}BAr'_4 (5), and $[Cp^*Ir(CO)H]_2$ (6)

	4	5[a]	5[a]	6
	Bond Lengths (Å)			
Ir(1)−Ir(2)	2.831(1)[b]	2.935(1)	2.921(1)	2.730(1)
Ir(1)−C(1)	1.857(12)	1.897(17)	1.887(12)	1.817(16)
Ir(2)−C(2)	1.869(13)	1.883(14)	1.856(16)	1.829(15)
Ir(1)−C(13)	2.034(9)			
Ir(2)−C(13)	2.028(9)			
Ir(1)−Cp(1)[c]	1.896	1.881	1.883	1.908
Ir(2)−Cp(2)	1.895	1.878	1.867	1.897
C(1)−O(1)	1.148(15)	1.099(20)	1.135(15)	1.158(19)
C(2)−O(2)	1.150(16)	1.119(17)	1.175(19)	1.150(18)
C(13)−O(3)	1.180(10)			
	Bond Angles (deg)			
Ir(1)−Ir(2)−Cp(2)	136.5	131.6	132.2	128.8
Ir(2)−Ir(1)−Cp(1)	137.1	131.8	130.6	129.9
Ir(1)−Ir(2)−C(2)	93.5(3)	77.8(4)	78.5(4)	85.1(5)
Ir(2)−Ir(1)−C(1)	93.4(3)	80.9(4)	82.0(4)	85.4(5)
Ir(1)−Ir(2)−C(13)	45.9(3)			
Ir(1)−C(13)−Ir(2)	88.4(3)			
Ir(1)−C(1)−O(1)	174.1(9)	179.4(15)	176.8(11)	179.0(6)
Ir(2)−C(2)−O(2)	175.7(10)	177.6(10)	176.6(11)	177.8(13)
Ir(1)−C(13)−O(3)	135.6(7)			
Ir(2)−C(13)−O(3)	136.1(8)			
Cp(1)−Ir(1)−C(1)	129.1	130.6	130.4	136.2
Cp(2)−Ir(2)−C(2)	129.5	134.0	131.6	136.0
	Dihedral Angles (deg)			
Cp(1)−Ir(1)−Ir(2)−Cp(2)	172.9	153.1	158.2	142.9
C(1)−Ir(1)−Ir(2)−C(2)	171.3	70.3	72.8	83.0

[a] Crystal structure of **5** consists of two unique molecules per asymmetric unit. [b] Standard deviations in the least significant figures are enclosed in parentheses following the value. [c] Cp(1) refers to the centroid of Cp attached to Ir(1).

electronic structure of piano-stool dimers, note that complexes of the form $[CpML]_2(\mu$-$L)_2$ "seem only able to form μ-H products if the bridging ligands transform to terminal ones". Examples include the protonation of $[CpFe(CO)]_2(\mu$-$CO)_2$[16] and $[CpRu(PMe_3)]_2(\mu$-$CO)_2$[17] to generate $[CpFe(CO)_2]_2(\mu$-$H)^+$ and $[CpRu(CO)(PMe_3)]_2(\mu$-$H)^+$, respectively. The relative stability of the bridged versus unbridged forms of the CpRh analogue, $Cp_2Rh_2(CO)_2$, have been calculated theoretically.[18] Though the bridged form $[CpRh(\mu$-$CO)]_2$ is more stable then the unbridged by 21.7 kcal/mol, the unbridged form is better suited to bind a proton (also CH_2 or CO). The stabilizing interaction of the incoming empty proton s-orbital with the HOMO of the unbridged $[Cp^*Ir(CO)]_2$ (metal−metal σ) favors formation of the μ-H product.

(15) Bursten, B. E.; Cayton, R. H. *J. Am. Chem. Soc.* **1987**, *109*, 6053.
(16) Legzdins, P.; Martin, D. T.; Nurse, C. R.; Wassink, B. *Organometallics* **1983**, *2*, 1238.
(17) Chinn, M. S. Ph.D. Thesis, Yale University, 1989.
(18) Pinhas, A. R.; Albright, T. A.; Hofmann, P.; Hoffmann, R. *Helv. Chim. Acta* **1980**, *63*, 29.

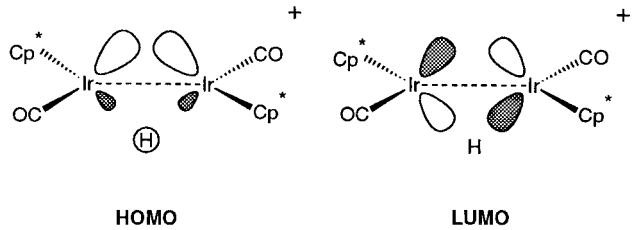

Figure 4. The frontier orbitals of $[Cp^*Ir(CO)]_2(\mu\text{-}H)^+$ (**2**).

On the basis of the molecular orbital diagrams for the interaction of $[CpM(CO)]_2$ (M = Co, Rh) and CH_2 fragments,[15,19] we can construct the frontier orbitals of the monoprotonated dimer **2**, using the related interaction of the $[Cp^*Ir(CO)]_2$ and H^+ fragment orbitals. In so doing, the dimer's enhanced reactivity becomes apparent. The HOMO is directed toward the empty bridging position, well-suited for a σ interaction (Figure 4). The LUMO is perfectly situated for a π interaction at the empty bridging position.[20] Rapid reaction of CO, H_2, or a second H^+ is in accord with this orbital description.

The protonation of **1** with $HBAr'_4 \cdot 2Et_2O$, as monitored by ^1H NMR, results in a much cleaner conversion to the monoprotonated dimer **2** than does HOTf, $HBF_4 \cdot Et_2O$, or $H_2C(SO_2CF_3)_2$. Some of the side products generated upon protonation of **1** with HOTf, $HBF_4 \cdot Et_2O$, or $H_2C(SO_2CF_3)_2$ are most likely due to interaction of the respective conjugate base with the empty bridging site, even though they are relatively poor ligands. The $BAr'_4{}^-$ anion was developed[21] as a truly noncoordinating counterion and its utility is borne out in this chemistry.

Reactions of $\{[Cp^*Ir(CO)]_2(\mu\text{-}H)\}BAr'_4$ (2-BAr′$_4$). As mentioned above, protonation of $[Cp^*Ir(\mu\text{-}CO)]_2$ (**1**) greatly increases its subsequent reactivity. An important example is the reaction with hydrogen. Addition of H_2 to dimers containing metal−metal multiple bonds often leads to cleavage of those bonds with concomitant formation of the corresponding monomeric hydrides. There are relatively few examples of unsaturated metal dimers which undergo oxidative addition of H_2 across the metal−metal multiple bond to generate stable dimeric dihydrides.[22−27] A tungsten dimer reported by Green and Mountford,[24] $[(\eta^5\text{-}C_5H_4{}^iPr)WCl_2]_2$, containing a formal W−W triple bond without bridging ligands, adds H_2 at room temperature to generate the doubly hydride-bridged $[(\eta^5\text{-}C_5H_4{}^iPr)WCl_2(\mu\text{-}H)]_2$. This was noted as the first case in which thermal H_2 addition across M−M multiple bonds was reversible. The concerted 1,2-dinuclear oxidative addition of H_2 to a bimetallic compound is forbidden due to orbital symmetry constraints,[28] just as it is for the reverse reductive-elimination reaction. Hence, these reactions are thought to proceed via initial addition of H_2 to a single metal center.

The dimer **1** does react with H_2 (P = 2.8 atm), but the reaction is sluggish, occurring over the course of several days. In addition, the Ir═Ir bond is broken, yielding the monomer, $Cp^*Ir(CO)H_2$, as the product. By comparison, **2** reacts completely with H_2 in several minutes. Moreover, the metal−metal bond remains intact as H_2 formally adds across the Ir═Ir bond to afford $[Cp^*Ir(CO)H]_2(\mu\text{-}H)^+$ (**5**). Of course, the Ir−Ir bond order in **2** is somewhat ambiguous due to the bridging hydride. The M−(μ-H)−M interaction is best described as a delocalized 3-center, 2-electron bond.[29] Since **2** can be prepared by addition of a proton (i.e., no electrons) to a compound containing an Ir═Ir double bond, it seems reasonable to postulate that multiple bond character is retained. An X-ray structure determination of $[Cp^*Ir(CO)]_2(\mu\text{-}H)^+$ furnishing an Ir−Ir bond length would be informative.

Perhaps the closest example to our system is provided by Casey and co-workers[25] who reported the rapid reaction of H_2 with $[Cp^*Re(CO)_2]_2$ (formal Re═Re double bond) to form $[Cp^*Re(CO)_2]_2(\mu\text{-}H)_2$. In this case, the facile addition of H_2 may be attributable to the fact that the carbonyls of $[Cp^*Re(CO)_2]_2$ are semibridging, i.e., that the Re═Re double bond is not entirely protected by the bridging carbonyls.

Like hydrogen, CO also reacts more rapidly with the monoprotonated dimer, **2**, than with **1**, though the advantage is less substantial. Carbon monoxide instantaneously adds to **2** to form $[Cp^*Ir(CO)]_2(\mu\text{-}CO)(\mu\text{-}H)^+$ (**4**). Carbonylation of **1** to form $[Cp^*Ir(CO)]_2(\mu\text{-}CO)$ requires 30 min for complete reaction.[6,30]

The formation of the dihydride dication $[Cp^*Ir(CO)]_2(\mu\text{-}H)_2{}^{2+}$ (**3**) from reaction of **1** with greater than 1 equiv of various strong acids was somewhat surprising since there are few reports of iridium hydride dications in the literature. Most cationic iridium hydride complexes are themselves acidic and hence are not amenable to protonation.

However, the reaction of $[Cp^*Ir(CO)]_2(\mu\text{-}H)^+$ (**2**) with a second proton is not surprising in light of the molecular orbital description. The HOMO of **2** points directly at the empty bridging position and is perfectly situated to interact with the incoming proton. The proposed structure of the dihydride dication, **3**, with trans Cp* ligands, terminal carbonyls, and bridging hydrides, would be isostructural to the isoelectronic osmium neutral complex $[Cp^*Os(CO)]_2(\mu\text{-}H)_2$.[31] There are many

(19) Hofmann, P. *Angew. Chem., Int. Ed. Engl.* **1979**, *18*, 554.

(20) The interaction of the HOMO and LUMO of $[Cp^*Ir(CO)]_2(\mu\text{-}H)^+$ (**2**) with a π acceptor like CO might appear at first glance to be unfavorable, since it would necessitate the interaction of two filled orbitals of σ symmetry as well as two empty orbitals of π symmetry. However, the bonding molecular orbital formed by interaction of the LUMO of **2** with the CO π^* orbital should be much lower in energy than the antibonding molecular orbital formed from combination of the HOMO of **2** and the CO σ orbital. Hence, the four available valence electrons will fill the two bonding MOs, yielding a favorable interaction. It is the distribution of the electrons in the final molecule that is important, not the arbitrary electron occupation of the conceptual fragments. For further explanation, see: Albright, T. A.; Burdett, J. K.; Whangbo, M.-H. *Orbital Interactions in Chemistry*; John Wiley and Sons: New York, 1985; p 406.

(21) Brookhart, M.; Grant, B.; Volpe, A. F., Jr. *Organometallics* **1992**, *11*, 3920.

(22) Sattelberger, A. P.; Wilson, R. B., Jr.; Huffman, J. C. *J. Am. Chem. Soc.* **1980**, *102*, 7111.

(23) Ting, C.; Baenziger, N. C.; Messerle, L. *J. Chem. Soc., Chem. Commun.* **1988**, 1133.

(24) Green, M. L. H.; Mountford, P. *J. Chem. Soc., Chem. Commun.* **1989**, 732.

(25) Casey, C. P.; Sakaba, H.; Hazin, P. N.; Powell, D. R. *J. Am. Chem. Soc.* **1991**, *113*, 8165.

(26) Chaudret, B.; Dahan, F.; Sabo, S. *Organometallics* **1985**, *4*, 1490.

(27) Field, J. S.; Haines, R. J.; Stewart, M. W.; Sündermeyer, J.; Woollam, S. F. *J. Chem. Soc., Dalton Trans.* **1993**, 947.

(28) Trinquier, G.; Hoffmann, R. *Organometallics* **1984**, *3*, 370.

(29) Bau, R.; Teller, R. G.; Kirtley, S. W.; Koetzle, T. F. *Acc. Chem. Res.* **1979**, *12*, 176.

(30) McGhee, W. D.; Foo, T.; Hollander, F. J.; Bergman, R. G. *J. Am. Chem. Soc.* **1988**, *110*, 8543.

(31) Hoyano, J. K.; Graham, W. A. G. *J. Am. Chem. Soc.* **1982**, *104*, 3722.

other transition metal dimers with M=M double bonds bridged by two hydride ligands,[32] formally "diprotonated double bonds", but none to our knowledge were actually generated by successive protonations of the metal−metal bond.

The ν_{CO} (2052 cm^{-1}) peak in the IR spectrum of **3-BF$_4$** is at the high end of the range for terminal CO stretching vibrations and indicates poor back-donation to the carbonyls, which is consistent with the dication formulation. In comparison, the terminal CO stretching frequency of the monocation **2** is 1994 cm^{-1} and those of the neutral dihydride dimer **6** are 1971 and 1942 cm^{-1}. The related dication $[Cp^*Ir(CO)_2]_2(BF_4)_2$ reported by Sutton and co-workers[33] also exhibits high ν_{CO} frequencies at 2073 and 2058 cm^{-1}. The single carbonyl band is again consistent with that predicted for a trans geometry of C_{2h} symmetry.

Solid State Structure of {[Cp*Ir(CO)H]$_2$(μ-H)}-BAr′$_4$ (5) and [Cp*Ir(CO)H]$_2$ (6). A single-crystal X-ray structure determination confirmed the dimeric nature of $[Cp^*Ir(CO)H]_2$ (**6**), with an Ir−Ir bond length of 2.730 Å and terminal carbonyl ligands (Figure 3).[34] Interligand angles in **6** are similar to those observed[35] in closely related pseudo-octahedral monomeric complexes such as $Cp^*Ir(PMe_3)(Cy)H$, in which, for example, the angles between the Cp* centroid (referred to as Cp^*_c) and the phosphine and between Cp^*_c and the cyclohexyl carbon are 131° and 129°, respectively. The comparable angles in **6** between Cp^*_c and the carbonyl group and between Cp^*_c and the distant iridium atom (Cp^*_c−Ir−Ir) are 136° and 129°, respectively. The Cp* rings of **6** are disposed in a transoid fashion, though the dihedral angle (142.9°) is somewhat less than 180° perhaps due to some steric interaction between the Cp* methyl groups and the carbonyl attached to the distant iridium atom. The Ir−C−O angles are essentially linear (179.0° and 177.8°).

While the hydride ligands of **6** could not be definitively located from the crystallographic analysis, the infrared spectrum (ν_{Ir-H} = 2180 cm^{-1})[8] supports a terminal hydride description. For comparison, structural characterization of $[Cp^*Os(CO)(\mu\text{-}H)]_2$, a complex of osmium with the same ligand set as **6**, indicates that the two hydride ligands are bridging the Os=Os double bond.[31] Significantly, in $[Cp^*Os(CO)(\mu\text{-}H)]_2$, the metal atoms, the carbonyl carbons, and the ring centroids all form a plane. In contrast, the asymmetry of the ancillary ligands of complex **6** again suggests that the hydride ligands occupy terminal positions. Placement of the hydride ligands in their expected positions, based on a pseudo-octahedral geometry about the iridium atoms, reveals that **6** has crystallized as the racemic diastereomer (*RR*/*SS* enantiomeric pair).

There are few examples of structurally characterized, unbridged Ir−Ir single bonds in the literature.[33,36−39] Examples include a distance of 2.717 Å reported[36] in 1973 for $Ir_2(NO)_4(PPh_3)_2$ and a distance of 2.839 Å reported[33] for the dication $[Cp^*Ir(CO)_2]_2^{2+}$. The mean Ir−Ir bond length of $Ir_4(CO)_{12}$, a tetrahedral cluster of four iridium atoms with terminal carbonyl ligands, is 2.68 Å,[40] but it is unclear whether this represents a true "unsupported" Ir−Ir single bond since each Ir−Ir bond is bridged by the two other iridium atoms.

Determination of the structure of {$[Cp^*Ir(CO)H]_2(\mu\text{-}H)$}BAr′$_4$ (**5**) by X-ray diffraction analysis (Figure 2) provides a unique opportunity to evaluate the effect of protonation upon the length of an unsupported metal−metal bond. This has not been determined previously for iridium. The crystal structure of **5** consists of two independent molecules, so mean values of the two will be used for comparison. The Ir−Ir bond length in **5** is 2.928 Å, which is significantly longer (by 0.198 Å) than that in $[Cp^*Ir(CO)H]_2$ (**6**). Churchill and co-workers[41] were the first to make the generalization that protonation of an unsupported metal−metal bond leads to an increase in the length of that metal−metal bond.[42] This is what we would expect based upon conversion from a 2-center, 2-electron bond to a delocalized 3-center, 2-electron bond. There are few examples in the literature wherein a complex containing an unsupported metal−metal bond and the corresponding complex containing the protonated metal−metal bond are both structurally characterized by diffraction methods. One of the first X-ray diffraction studies of polynuclear transition metal complexes containing a bridging hydride involved a pair of chromium dimers $[Cr_2(CO)_{10}]^{2-}$ and $[Cr_2(CO)_{10}(\mu\text{-}H)]^-$, which revealed a marked 0.44 Å increase in the Cr−Cr bond length upon protonation.[43] A complex containing a third row metal, $[Re_3(CO)_{12}(\mu\text{-}H)]^{2-}$, possesses a triangular metal core with one hydrogen-bridged Re−Re bond.[44] The Re−Re bond bridged by the hydride ligand is 0.14 Å longer than each of the unbridged Re−Re bonds, which is closer to the change in the metal−metal bond length we find in our system for iridium. Again, however, the nonhydride-bridged, Re−Re bonds are not truly "unsupported" as they are bridged by the third Re atom, and it is unclear what effect this has on the Re−Re bond lengths.

The hydride ligands of the trihydride cation dimer, **5**, were not located. The ligand bond angles of **5** are similar to those of the neutral dihydride dimer, **6**. The carbonyl carbons of **5** are bent slightly more toward the Ir−Ir bond, and the Cp* rings are disposed in a more

(32) Examples include: (a) Alt, H. G.; Mahmoud, K. A.; Rest, A. J. *Angew. Chem., Int. Ed. Engl.* **1983**, *22*, 544. (b) Mahmoud, K. A.; Rest, A. J.; Alt, H. G. *J. Chem. Soc., Dalton Trans.* **1985**, 1365. (c) Legzdins, P.; Martin, J. T.; Oxley, J. C. *Organometallics* **1985**, *4*, 1263. (d) Dahl, L. F. *Ann. N. Y. Acad. Sci.* **1983**, 1 and references therein.

(33) Einstein, F. W. B.; Jones, R. H.; Zhang, X.; Yan, X.; Nagelkerke, R.; Sutton, D. *J. Chem. Soc., Chem. Commun.* **1989**, 1424.

(34) The lower symmetry analogue, $[(\eta^5\text{-}C_5Me_4Et)Ir(CO)H]_2$, has an Ir−Ir bond length of 2.724(1) Å,[8] as determined by X-ray crystallography.

(35) The crystal structure of $Cp^*Ir(PMe_3)(Cy)H$ consists of two independent molecules; we report angles herein as mean values of the two, see: Buchanan, J. M.; Stryker, J. M.; Bergman, R. G. *J. Am. Chem. Soc.* **1986**, *108*, 1537.

(36) Angoletta, M.; Ciani, G.; Manassero, M.; Sansoni, M. *J. Chem. Soc., Chem. Commun.* **1973**, 789.

(37) Rasmussen, P. G.; Anderson, J. E.; Bailey, O. H.; Tamres, M.; Bayón, J. C. *J. Am. Chem. Soc.* **1985**, *107*, 279.

(38) Ciriano, M. A.; Sebastián, S.; Oro, L. A.; Tiripicchio, A.; Tiripicchio Camellini, M.; Lahoz, F. J. *Angew. Chem., Int. Ed. Engl.* **1988**, *27*, 402.

(39) Beringhelli, T.; Ciani, G.; D'Alfonso, G.; Garlaschelli, L.; Moret, M.; Sironi, A. *J. Chem. Soc., Dalton Trans.* **1992**, 1865.

(40) Wilkes, G. R. *Diss. Abstr.* **1966**, *26*, 5029.

(41) Churchill, M. R.; DeBoer, B. G.; Rotella, F. J. *Inorg. Chem.* **1976**, *15*, 1843.

(42) It has been reported that protonation of a Rh−Co bond leads to a *shortening* of that bond; however, the compound contains a semibridging CO which is believed to have a significant effect on the metal−metal bond length, see: Elliot, D. J.; Vittal, J. J.; Puddephatt, R. J.; Holah, D. G.; Hughes, A. N. *Inorg. Chem.* **1992**, *31*, 1247.

(43) Handy, L. B.; Ruff, J. K.; Dahl, L. F. *J. Am. Chem. Soc.* **1970**, *92*, 7312.

(44) Churchill, M. R. *Adv. Chem. Ser.* **1978**, *167*, 36.

nearly trans geometry (dihedral angle = 155.6°). The bonds between the iridium atoms and the carbonyl carbons of **5** are longer than the corresponding bonds in **6**, which is consistent with its positive charge and, hence, reduced back-donation from the iridium to the carbonyl π^* orbitals. There appears to be no interaction between the $BAr'_4{}^-$ anion and the iridium centers (closest contact >5 Å).

The structure of **5** can profitably be compared to that of the trimethylphosphine analogue $\{[Cp^*Ir(PMe_3)H]_2(\mu\text{-}H)\}PF_6$.[45] The Ir−Ir bond length in $[Cp^*Ir(PMe_3)H]_2(\mu\text{-}H)^+$ is 2.983 Å, slightly longer than the Ir−Ir bond of **5** (2.928 Å), and the hydrides were located, confirming the presence of two terminal and one bridging hydride. The configuration of the ligands around the iridium atoms in **5** is very similar to that of the phosphine analogue. Again, placement of the terminal hydride ligands in their expected positions, based on a pseudo-octahedral geometry (ignoring the bridging hydride ligand) about the iridium atoms (and based on comparison to $[Cp^*Ir(PMe_3)H]_2(\mu\text{-}H)^+$), reveals that **5** has crystallized as the racemic diastereomer (*RR*/*SS* enantiomeric pair).

Solid State Structure of $\{[Cp^*Ir(CO)]_2(\mu\text{-}CO)(\mu\text{-}H)\}OTf$ (4-OTf). The unusual manner in which this crystal was generated warrants comment. The partial decomposition of $\{[Cp^*Ir(CO)H]_2(\mu\text{-}H)\}OTf$ (**5-OTf**) to **4** and two other unidentified products occurs slowly (over the course of several months) in the solid state under argon. A plausible mechanism might involve slow loss of H_2 to form $[Cp^*Ir(CO)]_2(\mu\text{-}H)^+$ (**2**), followed by rapid scavenging of CO from another molecule of **5-OTf**. However, subjecting solid **5-OTf** to dynamic vacuum overnight produces no observed decomposition by ^1H NMR. A solution of **5-OTf** in $CDCl_2F$ kept in the freezer (−30 °C) for almost 2 years showed essentially no decomposition. Reversible H_2 addition across a metal−metal multiple bond would be intriguing, as we know of only two reported examples.[24,27]

The dimeric nature of **4** was confirmed by an X-ray structure determination (Figure 1). The Cp* ligands are disposed in a trans fashion (Cp^*_c−Ir−Ir−Cp^*_c dihedral angle = 173°), as are the terminal carbonyl ligands (C−Ir−Ir−C dihedral angle = 171°). The Ir−C−O angles are reduced slightly from 180° (174° and 176°) and are bent away from the vicinal Cp* ligand. The iridium atoms, the Cp* centroids, and the terminal carbonyl carbon atoms are all essentially coplanar. The bridging carbonyl makes an angle of approximately 90° with this plane and is symmetrically positioned between the Ir atoms. Though the hydride was not explicitly located, it seems apparent from the symmetry of the structure that the hydride occupies the empty bridging site opposite the carbonyl. The Ir−Ir bond length (2.831 Å) is consistent with an Ir−Ir single bond and is longer than that of the unsupported Ir−Ir bond in $[Cp^*Ir(CO)H]_2$ (**6**) (2.730 Å) but shorter than the hydride-bridged Ir−Ir bond in $\{[Cp^*Ir(CO)H]_2(\mu\text{-}H)\}BAr'_4$ (**5**) (mean 2.928 Å). This suggests that the bridging carbonyl holds the iridium atoms closer together than would be expected for a simple hydride-bridged dimer. The triflate anion is noncoordinating: the closest contact is 2.921 Å, between one of its oxygen atoms and a Cp* methyl hydrogen.

(45) Burns, C. J.; Rutherford, N. M.; Berg, D. J. *Acta Crystallogr., Sect. C* **1987**, *43*, 229.

Conclusion

The carbonyl-bridged dimer $[Cp^*Ir(\mu\text{-}CO)]_2$ (**1**) can be protonated by a variety of strong acids. Reaction of **1** with 1 equiv of $HBAr'_4{\cdot}2Et_2O$ opens the carbonyl bridges to generate $[Cp^*Ir(CO)]_2(\mu\text{-}H)^+$ (**2**) and substantially increases the reactivity of the dimer. The monoprotonated dimer, **2**, reacts rapidly at room temperature with H_2 or CO without cleavage of the metal−metal bond. The hydride cation dimer, **2**, can also react with a second equivalent of acid to yield the dihydride dication $[Cp^*Ir(CO)]_2(\mu\text{-}H)_2{}^{2+}$ (**3**). Addition of H_2 to **2** to form the trihydride dimer $[Cp^*Ir(CO)H]_2(\mu\text{-}H)^+$ (**5**) is an uncommon example of oxidative addition of H_2 across a metal−metal multiple bond, resulting in a stable dimeric product. The rapid, one-pot generation of complex **5** from **1**, $HBAr'_4{\cdot}2Et_2O$, and H_2 should prove to be a useful synthetic route to the hydride dimers. As expected, protonation of the unsupported Ir−Ir bond of $[Cp^*Ir(CO)H]_2$ (**6**) leads to the lengthening of that bond (by ca. 0.2 Å).

We speculate that addition of an acid with a noncoordinating anion, such as $HBAr'_4{\cdot}2Et_2O$, may prove to be a general route to enhanced reactivity in compounds with carbonyl ligands that bridge a metal−metal multiple bond.

Experimental Section

General Comments. All manipulations were conducted under argon and nitrogen using standard Schlenk and drybox techniques. Argon and nitrogen were deoxygenated and dried by passage through a Chemical Dynamics Corp. R3-11 CuO catalyst followed by Mallinckrodt Aquasorb containing P_2O_5. Air-sensitive compounds were manipulated in an MBraun labmaster 130 glovebox equipped with an integrated dry train loaded with copper catalyst and molecular sieves. Solvents were purified by distillation from Na/K/benzophenone (except CH_2Cl_2 from P_2O_5) under nitrogen. Deuterated NMR solvents (purchased from Cambridge Isotope Laboratories) were degassed and stored over the following drying agents: CD_2Cl_2, CD_3NO_2 over CaH_2; C_6D_6 over Na/K/benzophenone; $(CD_3)_2CO$ over molecular sieves (4 Å).

The dimers $[Cp^*Ir(\mu\text{-}CO)]_2$ (**1**)[3] and $[Cp^*Ir(CO)H]_2$ (**6**)[8] were prepared according to the published procedures. The acid $H_2C(SO_2CF_3)_2$ was the generous gift of Dr. Allen Siedle of 3M. $[Ph_3C]BAr'_4$[46] and $HBAr'_4{\cdot}2Et_2O$[21] were prepared by the reported methods.

^1H NMR spectra were recorded on Bruker AC200, AF300, or WM500 spectrometers and referenced internally to the residual proton resonance of the deuterated solvent or tetramethylsilane (TMS). Air-sensitive samples to be analyzed by NMR spectroscopy were prepared in Wilmad J. Young valve NMR tubes (equipped with a threaded Teflon piston, referred to herein as a "screw-cap" NMR tube) or flame-sealed in NMR tubes attached to Kontes high-vacuum Teflon stopcocks adapted for vacuum line connection.

$\{[Cp^*Ir(CO)]_2(\mu\text{-}H)\}BAr'_4$ (2) from $[Cp^*Ir(\mu\text{-}CO)]_2$ (1) and $HBAr'_4{\cdot}2Et_2O$. A Schlenk flask was charged with 20.2 mg of **1** (28.4 μmol). Methylene chloride (12 mL, distilled) was added via cannula to give a clear, yellow-brown solution, and the flask was immersed in an ice bath. A solution of $HBAr'_4{\cdot}2Et_2O$ (29.4 mg, 29.0 μmol, 1.0 equiv) in CH_2Cl_2 (3 mL) was added via cannula, immediately creating a deep blue color. The solution was stirred for 30 min and the solvent removed in vacuo, leaving a dark blue-green, air-sensitive solid. The protonated dimer, **2**, is insoluble in C_6D_6, decomposes slowly (days) in CD_2Cl_2, and reacts instantly with CD_3NO_2 and

(46) Bahr, S. R.; Boudjouk, P. *J. Org. Chem.* **1992**, *57*, 5545.

acetone-d_6. ^{1}H NMR (CD_2Cl_2): δ 1.96 (Cp*, 30 H), −17.96 (Ir−H, 1 H). IR (Nujol): 1994 cm^{-1} (ν_{CO}).

Reaction of [Cp*Ir(μ-CO)]$_2$ (1) with HBF$_4$·Et$_2$O. An NMR tube fitted with a high-vacuum Teflon stopcock was charged with 2.9 mg of **1** (4.1 μmol). Methylene chloride-d_2 (0.4 mL) was added to the solids via vacuum transfer, yielding a yellow solution containing some brown insoluble material. With the solution immersed in a CO_2/IPA bath, ca. 1.0 μL of HBF$_4$·Et$_2$O (85%, 5.8 μmol, 1.4 equiv) was added via syringe against an argon purge. Three freeze/pump/thaw cycles were performed, and the tube was sealed under vacuum. Upon thawing, red-orange crystals precipitated from the brown-yellow liquid. A ^{1}H NMR spectrum revealed that the starting material had been entirely consumed and six new peaks appeared in the Cp* region as well as two peaks in the hydride region. Two resonances of approximately equal intensity at δ 2.11 and 1.99 account for 72% of the total Cp* region intensity. The resonances at δ 1.99 (30 H) and −17.94 (1 H) are attributed to the monoprotonated dimer, **2-BF$_4$**, by comparison to those of the BAr′$_4^-$ analogue. The resonances at 2.11 ppm (15 H) and −14.87 ppm (1 H) are tentatively assigned to the dication {[Cp*Ir(CO)]$_2$(μ-H)$_2$}(BF$_4$)$_2$ (**3**) by comparison to the BAr′$_4^-$ analogue. The red solid is believed to be the bulk insoluble fraction of **3**.

Reaction of [Cp*Ir(μ-CO)]$_2$ (1) with HOTf. The same procedure was used as that described above for HBF$_4$·Et$_2$O. In this case, 4.3 mg of **1** (6.1 μmol) and 1.0 μL of HOTf (2.0 equiv) were employed. The reaction furnished a green liquid over red solids. A ^{1}H NMR (CD_2Cl_2) spectrum displayed weak signal intensities, indicating that the majority of organometallic product is insoluble. The major soluble product is the monoprotonated dimer, **2-OTf** (δ 1.98, −17.94). These peaks are somewhat broadened, presumably due to intermolecular proton transfer. The monomer [Cp*Ir(CO)$_2$H]OTf[47] (δ 2.41, −13.8) is present as a minor product, as well as several unidentified species.

Reaction of [Cp*Ir(μ-CO)]$_2$ (1) with H$_2$C(SO$_2$CF$_3$)$_2$. To a screw-cap NMR tube charged with **1** (5.8 mg, 8.2 μmol) was added 4.4 mg of H$_2$C(SO$_2$CF$_3$)$_2$ (15.7 μmol, 1.9 equiv). Methylene chloride-d_2 (0.4 mL) was added to the solids via vacuum transfer. Upon thawing, the solution was immediately a deep blue-green. Over the course of 10−20 min, the solution became yellow-brown with dark solids. ^{1}H NMR spectroscopy revealed several new resonances, none of which were attributable to the monoprotonated dimer, **2**.

Reaction of [Cp*Ir(μ-CO)]$_2$ (1) with HCl. The same procedure was used as that described above for HBF$_4$·Et$_2$O. In this case, 3.3 mg of **1** (4.6 μmol) and 9 μL of anhydrous HCl (1.0 M in Et$_2$O, 2 equiv) were employed. No color change was observed, and a ^{1}H NMR spectrum indicated that no reaction had occurred upon standing for 3 days.

Reaction of {[Cp*Ir(CO)]$_2$(μ-H)}BAr′$_4$ (2) with [PPN]Cl. The protonated dimer, **2**, was generated in situ as follows: to an NMR tube fitted with a high-vacuum Teflon stopcock was added 3.1 mg of **1** (4.4 μmol) and 4.9 mg of HBAr′$_4$·2Et$_2$O (4.8 μmol, 1.1 equiv) in the glovebox. Methylene chloride was vacuum-transferred onto the solids, and the solution immediately became a deep blue-green color upon warming to room temperature. After the solution was allowed to stand at room temperature for 5−10 min, the tube was immersed in an ice bath and the solvent was removed in vacuo. In the glovebox, 2.9 mg of [PPN]Cl (5.0 μmol, 1.2 equiv) was added to the dark blue-green residue. CD_2Cl_2 was added to the solids via vacuum transfer, yielding an orange solution with some dark solids. The tube was sealed under vacuum, and a ^{1}H NMR spectrum was acquired. The primary Cp*-bearing product is **1** (δ 1.76). A peak at 1.55 ppm is assigned to HCl. There are four other small unidentified resonances in the Cp* region.

Reaction of [Cp*Ir(CO)H]$_2$ (6) with [Ph$_3$C]BAr′$_4$. To an NMR tube fitted with a high-vacuum Teflon stopcock was added 4.5 mg of **6** (6.3 μmol) and 7.7 mg of [Ph$_3$C]BAr′$_4$ (7.0 μmol, 1.1 equiv) in the glovebox. Methylene chloride-d_2 (0.4 mL) was vacuum-transferred onto the solids. The NMR tube was sealed under vacuum. The solution immediately became a deep blue-green color upon warming to room temperature. The major products were identified by ^{1}H NMR as **2** and Ph$_3$CH (δ 5.55 (Ph$_3$C*H*)). A small quantity of [Cp*Ir(CO)H]$_2$(μ-H)$^+$ (**5**) was also formed. Several small resonances (δ 1.97, 1.94, −18.05) were unidentified.

Reaction of {[Cp*Ir(CO)]$_2$(μ-H)}BAr′$_4$ (2) with CO. The protonated dimer, **2**, was generated in situ as follows: to a screw-cap NMR tube charged with **1** (6.3 mg, 8.9 μmol) was added 9.7 mg of HBAr′$_4$·2Et$_2$O (9.6 μmol, 1.1 equiv) in the glovebox. Methylene chloride-d_2 (0.5 mL) was added to the solids via vacuum transfer, yielding a dark blue-green solution. The NMR tube was immersed in a liquid N_2 bath, and the frozen solution was degassed. The entire NMR tube was immersed in a CO_2/2-propanol bath and pressurized to 1000 Torr (1.3 atm) with CO. Upon warming to room temperature (P_{298K} = 2.0 atm), the solution immediately became orange-brown. The major product was identified as {[Cp*Ir(CO)]$_2$(μ-CO)(μ-H)}BAr′$_4$ (**4**) based upon comparison to the ^{1}H NMR of **4-CH(SO$_2$CF$_3$)$_2$**. ^{1}H NMR (CD_2Cl_2) δ: 2.12 (s, Cp*, 30 H), −13.34 (s, Ir−H, 1 H).

Reaction of {[Cp*Ir(CO)]$_2$(μ-H)}BAr′$_4$ (2) with H$_2$. The protonated dimer, **2**, was generated in situ as follows: a screw-cap NMR tube was loaded with 3.6 mg of **1** (5.1 μmol) and 5.4 mg of HBAr′$_4$·2Et$_2$O (5.3 μmol, 1.1 equiv) in the glovebox. Methylene chloride-d_2 (0.4 mL) was added to the solid via vacuum transfer, and the solution was kept frozen. With the NMR tube completely immersed in a liquid N_2 bath, the head space was evacuated and subsequently pressurized to 561 Torr (0.74 atm) with H_2. The NMR tube was warmed to room temperature (P_{298K} = 2.9 atm), and the solution immediately became dark blue-green. After 5−10 minutes of gentle shaking, the solution became golden yellow. The predominant product was the trihydride cation dimer, **5**. A minor impurity at δ 1.79 was unidentified.

{[Cp*Ir(CO)]$_2$(μ-H)$_2$}(BF$_4$)$_2$ (3). A Schlenk flask was charged with 21.6 mg of **1** (30.4 μmol). Methylene chloride (10 mL, distilled) was added via cannula to give a yellow-brown solution containing some undissolved solid. In a separate Schlenk flask, a solution of 50 μL of HBF$_4$·Et$_2$O (85%, 9.5 equiv) in 5−10 mL of CH_2Cl_2 was prepared. The acid solution was subjected to three freeze/pump/thaw cycles, and the flask then immersed in an ice bath. The iridium solution was transferred via cannula to an addition funnel and added dropwise to the cold stirring acid solution. The addition produced a suspension of fine red solids in the pale orange liquid. The solution was allowed to stand overnight at −30 °C to encourage solid formation. The supernatant was removed via cannula, and the red solid was washed with 2 × 5 mL of cold CH_2Cl_2 (washings were pale blue, indicating some deprotonation of the product, presumably by adventitious water). Despite drying the air-sensitive product in vacuo for several hours, it was found to be sticky and difficult to manipulate, precluding a yield measurement. The product is insoluble in C_6D_6 and 1,2-difluorobenzene, slightly soluble in CD_2Cl_2, and reacts with CD_3NO_2 and $(CD_3)_2CO$. ^{1}H NMR (CD_2Cl_2): δ 2.11 (Cp*, 30 H), −14.87 (Ir−H, 2 H). IR (Nujol): 2052 cm^{-1} (ν_{CO})

Reaction of [Cp*Ir(μ-CO)]$_2$ (1) with excess HBAr′$_4$·2Et$_2$O. To a screw-cap NMR tube charged with **1** (3.5 mg, 4.9 μmol) was added 21.7 mg of HBAr′$_4$·2Et$_2$O (21.4 μmol, 4.3 equiv) in the glovebox. Methylene chloride-d_2 (0.4 mL) was added to the solids via vacuum transfer. Upon thawing, a deep blue-green solution was immediately formed. After 1−2 min of shaking, the color became red-brown. The principal product was the dication, **3-BAr′$_4$**. ^{1}H NMR: δ 2.01 (Cp*, 30 H), −15.23 (Ir−H, 2 H). A small peak at δ 1.95 is attributed to **2**

(47) Plank, J.; Riedel, D.; Herrmann, W. A. *Angew. Chem., Int. Ed. Engl.* **1980**, *19*, 937.

(the hydride could not be detected). Two other minor resonances in the Cp* region at δ 1.90 and 1.78 are unidentified. The dihydride dication, **3-BAr′$_4$**, completely decomposed upon standing in CD_2Cl_2 at room temperature overnight.

Reaction of {[Cp*Ir(CO)]$_2$(μ-H)$_2$}(BAr′$_4$)$_2$ (3) with 1,8-Bis(dimethylamino)naphthalene. The diprotonated dimer, **3**, was generated in situ as follows: a screw-cap NMR tube was loaded with 4.5 mg of **1** (6.3 μmol) and 25.8 mg of HBAr′$_4$·2Et$_2$O (25.5 μmol, 4.0 equiv) in the glovebox. Methylene chloride (0.6 mL) was added to the solids via vacuum transfer. The NMR tube was allowed to stand in an ice bath for 1 h, yielding a clear deep red solution. The volatiles were removed in vacuo, leaving an oily, red-orange residue. In the glovebox, 1,8-bis(dimethylamino)naphthalene (Proton Sponge, 19.1 μmol) was added to the residue. Methylene chloride-d_2 was added via vacuum transfer, yielding a deep green solution. The predominant organometallic product, as determined by ^{1}H NMR, was the monoprotonated dimer, **2**, along with formation of the protonated 1,8-bis(dimethylamino)naphthalene.

X-ray Structure Determination of {[Cp*Ir(CO)]$_2$(μ-CO)(μ-H)}OTf (4-OTf). A crystal of **4-OTf** was generated unintentionally in an attempt to grow X-ray diffraction quality crystals of {[Cp*Ir(CO)H]$_2$(μ-H)}OTf (**5-OTf**). A 5 mm glass tube sealed at one end and equipped with a high-vacuum Teflon stopcock was charged with 15.3 mg of **5-OTf**. This sample of **5-OTf** had been standing in the glovebox for 5 months and had decomposed slightly, as indicated by its color change from pale to dark brown and by a ^{1}H NMR (CD_2Cl_2) spectrum which exhibited three new resonances of weak intensity in the Cp* region, one of which we attribute to **4-OTf**. A small quantity of acetone was added to the trihydride, **5-OTf**, via vacuum transfer, yielding a clear brown solution. A greater quantity of pentane was layered onto the solution via vacuum transfer, and the tube was sealed under vacuum. Crystals of **4-OTf** were formed amidst brown amorphous solids after standing for a week in the dark.

A clear orange-red crystal was mounted in a stream of nitrogen gas at 183 K on an Enraf-Nonius CAD-4 diffractometer. Systematic absences were consistent with the monoclinic space group $P2_1/n$. A total of 4752 independent reflections were collected with $2\theta \leq 50°$, of which 3515 with $I > 4\sigma(I)$ were used in the refinement. The structure was solved by direct methods, which gave the location of the Ir atoms. The remaining non-hydrogen atoms were located from difference Fourier maps. The hydrogen atoms were placed at calculated positions. The hydride bound to iridium was not located. The final R factor was 3.58%.

X-ray Structure Determination of {[Cp*Ir(CO)H]$_2$(μ-H)}BAr′$_4$ (5-BAr′$_4$). Crystals were generated from a saturated solution of **5** in CD_2Cl_2 upon standing overnight at −30 °C in a sealed 5 mm tube. The tube was cracked under a blanket of argon, and the crystals were shaken into a petri dish containing heavy paraffin oil. A green trapezoidal plate was mounted in a stream of nitrogen gas at 183 K on an Enraf-Nonius CAD-4 diffractometer. The data were collected for a triclinic cell, and the assigned space group was $P\bar{1}$. The unit cell contained two unique molecules, with only slight structural differences. A total of 14 536 independent reflections were collected with $2\theta \leq 45°$, of which 10 793 with $I > 4\sigma(I)$ were used in the refinement. The structure was solved primarily from the Patterson map. The remaining non-hydrogen atoms were located from difference Fourier maps. The hydrogen atoms were placed at calculated positions. Hydrides bound to iridium were not located. The final R factor was 4.48%.

X-ray Structure Determination of [Cp*Ir(CO)H]$_2$ (6). The crystal was generated via sublimation at 96 °C in an NMR tube which had been flame-sealed under vacuum. After the tube was heated overnight, large yellow crystals of **6** had sublimed onto the sides of the NMR tube, just above the level of the sand bath. The tube was cracked under a flow of argon, and the crystals were shaken into a petri dish containing heavy paraffin oil. One such crystal was mounted in a stream of nitrogen gas at 183 K on an Enraf-Nonius CAD-4 diffractometer. Systematic absences were consistent with the orthorhombic space group *Pbca*. A total of 3817 independent reflections were collected with $2\theta \leq 50°$, of which 2275 with $I > 4\sigma(I)$ were used in the refinement. The structure was solved by direct methods, which gave the location of the Ir atoms. The remaining non-hydrogen atoms were located from difference Fourier maps. The hydrogen atoms were placed at calculated positions. Hydrides bound to iridium were not located. The final R factor was 3.75%.

Acknowledgment. We thank the National Science Foundation for support of this research. We gratefully acknowledge Dr. K. I. Goldberg and Dr. B. E. Bursten for helpful discussions.

Supporting Information Available: Tables of structure determination summaries, bond lengths and angles, atomic coordinates, and thermal parameters for **4**, **5**, and **6** and ORTEP diagrams for **4** and **5** (38 pages). Ordering information is given on any current masthead page.

OM961103M